DENOISING THE SHOCKWAVE PRESSURE SIGNAL OF UNDERWATER EXPLOSION BASED ON EMD-CEEMDAN IN CONSIDERATION OF THE SIGNAL CURVE CURVATURE

Tung Lam Vu[1,*], Trong Thang Dam[1], Duc Viet Tran[2]

[1]*Le Quy Don Technical University, Hanoi, Vietnam*

[2]*General Department of Defence Industry, Hanoi, Vietnam*

Abstract

The measured signal of shockwave pressure of underwater explosion is usually disturbed by many objective factors such as the disturbance of the environment surrounding the sensors, the complexity of wave propagation and wave reflection in complex environments, the formation and fluctuation of air bubbles, especially analog signals always have noise due to the influence of electronic noise from the A/D converter and circuit board error embedded in measuring devices, etc. These are the main causes of initial waveform distortion, obscuring important characteristics of the signal, and making it difficult to use and further analyze underwater explosion shockwave pressure. Based on two algorithms Empirical Mode Decomposition (EMD) and Complete Ensemble Empirical Mode Decomposition with Adaptive Noise (CEEMDAN), this article combines the two algorithms above into one denoising model called EMD-CEEMDAN model with Python codes. Three evaluation criteria such as the average curvature of the signal curve, signal-to-noise ratio (SNR) and mean squared error (MSE) are applied to establish the most suitable denoising model. Applying this model to experimentally measured signal of underwater explosion shockwave pressure, the results show that high-frequency noise is eliminated, the denoised signal is transformed into a typically smooth explosion signal while its peak pressure value differs only about 2% from that of the initial signal.

Keywords: *Underwater explosions (UNDEX); denoising; EMD; CEEMDAN.*

1. Introduction

The use of explosive energy to break rock and soil has saved a large amount of time, effort, and money so far, as shown by the coal industry in Vietnam annually using thousands of tons of explosives. However, the best explosives in recent years, in terms of explosion efficiency, have only about 20% of the explosive energy becomes useful power in destroying rock and soil [1, 2], the rest of that affects the surrounding environment in the form of heat and vibration. Controlling blasting energy to serve the purpose of

*Email: lamvt@lqdtu.edu.vn

DOI: 10.56651/lqdtu.jst.v6.n02.745.sce

breaking rock and soil at will while limiting negative impacts on the environment or structures surrounding the blast is an important research area in blasting work.

To evaluate the impacts of blasting on the environment or structures near the explosion, current research is divided into two main directions. The first one is simulation by software. G. Barras et al. [3] modeled the dynamic effect of the air bubble of an underwater explosion; Emamzadeh et al. [4] studied the near-field blast wave propagation and its impact on structures; Huang et al. [5] studied the effect of explosion direction when blasting in water; R. Kicínski and B. Szturomski [6] described and synthesized in relative detail the phenomena related to underwater explosion waves and their effects on structures by simulation on the CAE software family; Peng et al. [7] performed numerical simulations of structural damage caused by near-field underwater explosions. Research in this direction mainly analyzes the dynamic response of structures when affected by underwater explosions based on numerical simulation using finite elements method (FEM) and the ALE method to calculate the dynamics phenomena in structures.

Using devices to directly measure explosion parameters is the second one. Research in this direction is inclined to analyze the dynamic effects of the blasting load itself, expressed by the parameters of the explosion. S. Beji et al. [8] performed underwater explosion pressure measurements to calculate new coefficients for the formula calculating the maximum pressure of incident waves; D. T. Thang et al. [9-11] conducted numerous experiments measuring many parameters of the explosion, including underwater shockwave pressure.

According to the second research direction, the complexity and difficulty in performing experiments and deploying measuring equipment to obtain data is uncontroversial, it takes a huge amount of effort and money, but it helps people best understand the physical nature of an explosion. The obtained measurement data is usually disturbed by the disturbance of the environment surrounding the sensors, the complexity of wave propagation and wave reflection in complex environments, the formation and fluctuation of air bubbles [12-14], especially analog signals always have noise due to the influence of electronic noise from the A/D converter and circuit board error embedded in measuring devices, etc. These are the main reasons leading to the distortion of the initial waveform, obscuring important characteristics of the explosion signal, making it difficult for further analysis. Therefore, the explosion signal needs to be denoised. Traditional noise reduction methods are spectrum analysis based on Fourier transform to remove high-frequency noise [15], using the Kalman filter algorithm that takes advantage of the signal delay to remove noise [16, 17]. The wavelet transform uses a mother waveform to

remove noise [18]. However, the characteristic of shockwave pressure of underwater explosion is a type of non-stationary random signal, with the characteristic of instantaneous frequency changing suddenly in an extremely short time, so traditional noise reduction methods seem to be inefficient.

Fortunately, with the development of science and technology in the 21st century and the 4.0 industrial revolution, new noise reduction methods have been introduced to replace traditional methods. Among them, EMD [19] and its advanced algorithms prove effective when showing superior abilities of noise cancellation while still retaining important information of the original signal. Sun et al. [12], Peng et al. [13], Liu and Peng [14] researched and built models based on EEMD, CEEMDAN (improved algorithms of EMD) to denoise blasting vibration, obtaining remarkable results. In the above studies, the authors also admitted that the new results were only suitable for signals measuring blasting vibrations with sensors placed on shore.

This article studies the use of the EMD-CEEMDAN algorithm for pieces of data in consideration of the curve curvature and some evaluation indices to denoise the shockwave pressure signal induced by underwater explosions. The results show an effective noise reduction ability while retaining the characteristics of the blast wave.

2. Noise reduction based on empirical mode decomposition

2.1. Empirical mode decomposition (EMD)

EMD was proposed by Huang et al. [19] to decompose the signal into Intrinsic Mode Functions (IMF). Flowchart of EMD algorithm is shown in Fig. 1.

In Fig. 1, $S(t)$ at steps 1 and 9 is the original signal; $s(t)$ at other steps is a continuously updated signal through iterations, set $s(t) = S(t)$ for the first time; $E_{max}(t)$, $E_{min}(t)$ are envelopes with the type of Akima spline connecting local maxima (upper envelope) and local minima (lower envelope) of $s(t)$, respectively; $E_{mean}(t)$ is the mean of two envelopes; r is the residue.

Checking IMF in step 5 consists of 2 conditions: In the first one, the number of extrema and that of zero-crossing points should be equal or different by at least 1; the second one is that the mean values of the upper and lower envelopes are equal to 0 at every point. The stopping criterion at step 8 is reached when r has no more than 2 extrema.

Generally speaking, the processing procedure of EMD algorithm includes 9 steps as follows: Step 1 - Load the input signal. Step 2 - Calculate the upper and lower envelopes of the signal $s(t)$ from the local extrema. Step 3 - Calculate the average from the upper and lower envelopes. Step 4 - Subtract the average from the original signal,

obtain $h(t)$. Step 5 - Check whether the obtained $h(t)$ is an IMF, if true, save it as the i^{th} IMF (step 6), if false, go back to step 2 but the new signal is now $h(t)$. Step 7 - Calculate the residual signal r. Step 8 - Check the stopping criterion, if true, stop the algorithm, the result now includes IMFs and a residue r, if false, return to step 2 with a new signal $h(t)$. The process from steps 2 to 6 is the most important process to extract the IMFs of EMD which is called sifting process.

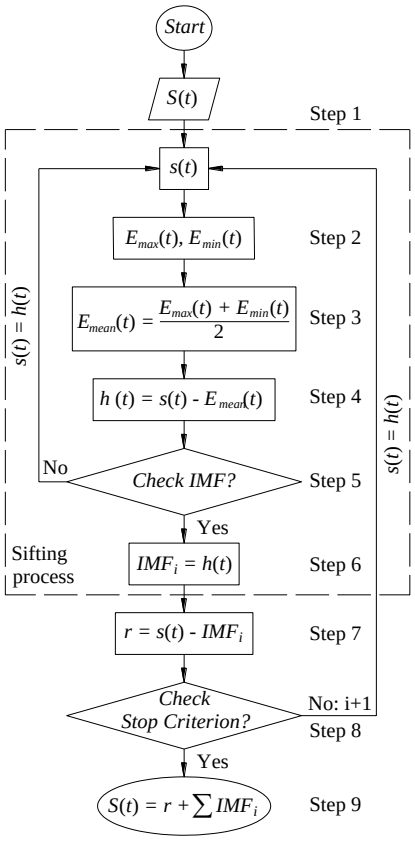

Fig. 1. EMD Flowchart.

2.2. Advanced algorithms of EMD

The decomposition results from EMD algorithm will create mode mixing, meaning the appearance of oscillations with very different amplitudes in one mode or the same oscillations appearing in different modes, causing difficulties for noise reduction [12].

To overcome this problem, Torres et al. [20] proposed Complete Ensemble Empirical Mode Decomposition with Adaptive Noise (CEEMDAN) with the ability to accurately reconstruct the original signal. CEEMDAN adds multiple white noises with different amplitudes to the original signal, performs EMD many times, and then calculates the average values at every step.

3. Curvature of a curve

The efficiency of denoising signal is equal to smoothing the signal curve, in nature. Figure 2 is a visualization of spline curvature with curvature combs and the way they change along the curve. In Fig. 2, curvature combs are perpendicular to the curve at every point. The magnitude of a curvature comb, which equals the inverse of the curve radius, is the curve curvature at that point. The curvature envelope helps us easily understand the curved characteristics of a curve.

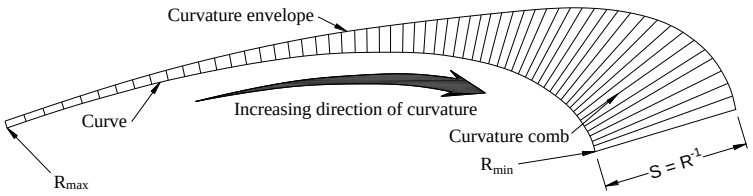

Fig. 2. Curvature Visualization of a curve.

As can be seen from Fig. 2, the curve radius and the curvature of every point are inversely proportional, which means that when the radius R is extremely small, the curvature C is extremely large, representing a point. By contrast, when the radius R is extremely large, the curvature C approaches 0, representing a straight line. Thus, the smoother the curve, the smaller the curvature.

Based on the visual representation of the curve above, this article proposes a way to evaluate the shockwave pressure signal curve as follows: Consider 3 consecutive points in the signal as points *i*-1, *i*, *i*+1, respectively. Determine the x and y-axis coordinates as the time values (seconds) and wavefront overpressure values (MPa), respectively, which are obtained from the measurement device. From the determined coordinates, calculate whether these 3 points belong to the same straight line by Eq. (1):

$$\left(x_{i-1}-x_i\right)\left(y_i-y_{i+1}\right)-\left(x_i-x_{i+1}\right)\left(y_{i-1}-y_i\right) \tag{1}$$

If the result from Eq. (1) is 0, then the 3 points under consideration are collinear, returning the curvature C_i at point i as 0. If the result calculated from Eq. (1) is different from 0, then the coordinates of the center point according to the x and y axes of the circumcircle of 3 points are calculated, corresponding to Eq. (2) and Eq. (3) as follows:

$$cx=\frac{\left[\left(x_{i-1}^2+y_{i-1}^2\right)-\left(x_i^2+y_i^2\right)\right]\left(y_i-y_{i+1}\right)-\left[\left(x_i^2+y_i^2\right)-\left(x_{i+1}^2+y_{i+1}^2\right)\right]\left(y_{i-1}-y_i\right)}{2\left[\left(x_{i-1}-x_i\right)\left(y_i-y_{i+1}\right)-\left(x_i-x_{i+1}\right)\left(y_{i-1}-y_i\right)\right]} \tag{2}$$

$$cy=\frac{\left(x_{i-1}-x_i\right)\left[\left(x_i^2+y_i^2\right)-\left(x_{i+1}^2+y_{i+1}^2\right)\right]-\left(x_i-x_{i+1}\right)\left[\left(x_{i-1}^2+y_{i-1}^2\right)-\left(x_i^2+y_i^2\right)\right]}{2\left[\left(x_{i-1}-x_i\right)\left(y_i-y_{i+1}\right)-\left(x_i-x_{i+1}\right)\left(y_{i-1}-y_i\right)\right]} \tag{3}$$

Curvature C_i at point i, in case that 3 points under consideration are not collinear, is calculated according to Eq. (4):

$$C_i = \frac{1}{\sqrt{\left(cx - x_{i-1}\right)^2 + \left(cy - y_{i-1}\right)^2}} \tag{4}$$

Averaging all calculated curvature values, the average curvature $\bar{C}_{signal}$ of the entire signal is obtained, expressed by Eq. (5) as follows:

$$\bar{C}_{signal} = \frac{1}{n-2}\sum_{i=2}^{n-1} C_i, \quad (n \geq 3) \tag{5}$$

where $\bar{C}_{signal}$ is the average curvature of the entire signal; C_i is the curvature of point i; n is the total number of signal points. In expression (5), the curvature is calculated for n-2 signal points to avoid the circumstance that the value of the calculation process exceeds the limit length of the signal.

4. Denoising signal of underwater shockwave pressure

4.1. Experiments on site

Experiments are carried out in a water pool with the shape of (6 × 6 × 2) m. TNT 5 g - 10 g is considered as explosives in experiments and detonated every charge per time with 1 gram detonator. The water height W is 1.95 m, the explosive charge and the sensor are placed on a plane parallel to the bottom with a distance is 0.8 m from the bottom. The sensor for measuring underwater shockwave pressure is the type of W138A05 from the PCB Piezotronics brand. The data is obtained and analyzed by the multi-channel measurement instrument DEWE-3020.

Experimental model is shown in Fig. 3.

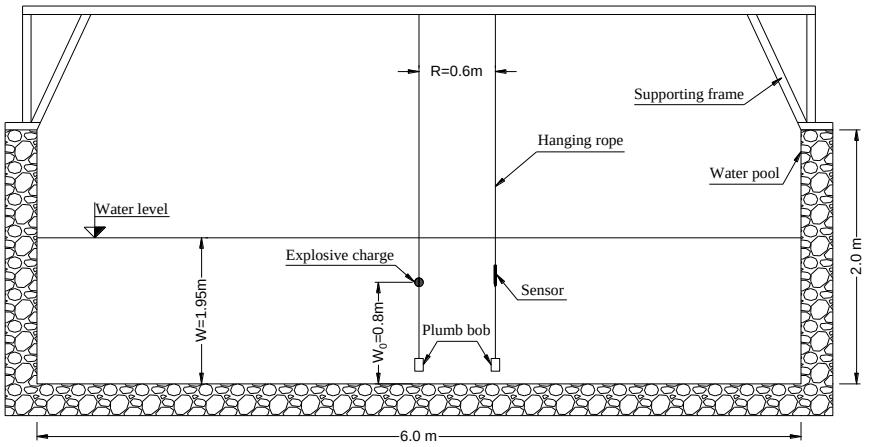

Fig. 3. The experimental model.

4.2. Theoretical parameters of the underwater explosion

According to Cole [21], an American scientist, formulas calculating the maximum pressure on the front of shockwave $p_{\max}$ and its time course $p(t)$ are as follows:

$$p_{\max} = 52.3\left(\frac{\sqrt[3]{C}}{R}\right)^{1.13}, \quad (\text{MPa}) \tag{6}$$

$$p(t) = p_{\max} e^{-\frac{t}{\theta}}, \quad (\text{MPa}) \tag{7}$$

where C is the charge mass (kg); R is the distance from the charge to the sensor (m); t is time (ms); θ is exponent time constant (ms). θ can be calculated through Eq. (8) as follows:

$$\theta = 0.093\sqrt[3]{C}\left(\frac{\sqrt[3]{C}}{R}\right)^{-0.22}, \quad (\text{ms}) \tag{8}$$

From Eq. (7), it can be seen that when $p(t)$ is set to 0, t will be the duration of positive phase of pressure pulse which is called τ^+. Calculating essential parameters from Eq. (6) and Eq. (8), and substituting them into Eq. (7), τ^+ is obtained.

4.3. Experimental results

Data of the first four underwater explosions are shown in Table 1 as follows:

Table 1. Experimental data

No.	C (kg)/ R (m)	Obtained from measured data		Calculated from (6), (7), (8)		
		p_{max} (MPa)	τ^+ (ms)	p_{max} (MPa)	Θ (ms)	τ^+ (ms)
1	0.006/ 0.6	7.697	0.730	13.561	0.022	0.210
2	0.006/ 0.6	6.110	0.720	13.561	0.022	0.210
3	0.011/ 0.6	11.673	0.775	17.039	0.026	0.262
4	0.011/ 0.6	13.134	0.780	17.039	0.026	0.262

In Table 1, C is the total mass of charge and detonator (kg); R is the distance from charge to sensor (m); $p_{\max}$ is the peak pressure of incident wave (MPa); τ^+ is duration of positive phase of pressure pulse (ms). For τ^+ in the "Obtained from measured data" column, the total number of samples, from the sample point which occurs the sudden increase of pressure to the sample point which has the first zero-crossing, is calculated by a simple counting algorithm, then it is multiplied by the sampling cycle, obtaining τ^+.

4.4. Data analysis and denoising process

4.4.1. Data analysis

According to the Nyquist sampling theorem, the sample rate of a periodic signal

must be at least twice its frequency to avoid a type of distortion called aliasing. Y. You and L. Li [22] specified that the dominant frequency of underwater blast wave signals is mainly concentrated around 50 kHz. Therefore, the chosen sampling frequency of 200 kHz in this study is suitable.

The underwater shockwave pressure signal of the first four blasting in the Table 1 is shown in Fig. 4. From Table 1, Fig. 4 and intuitively considering the signal waveform, it can be seen that the peak pressure of the incident wave changes suddenly with very large amplitude in an extremely short duration, only about 4 - 5 sampling times (corresponding to a time interval of 0.02 - 0.025 ms), causing a significant swing at the points where there should be no fluctuations, this also known as the end effect of EMD. To avoid this phenomenon, therefore, this article also establishes an algorithm detecting the points that are the beginning of pressure jumps J_i and the points that have peak pressures P_i, dividing the original signal into pieces of signal for separately denoising purposes.

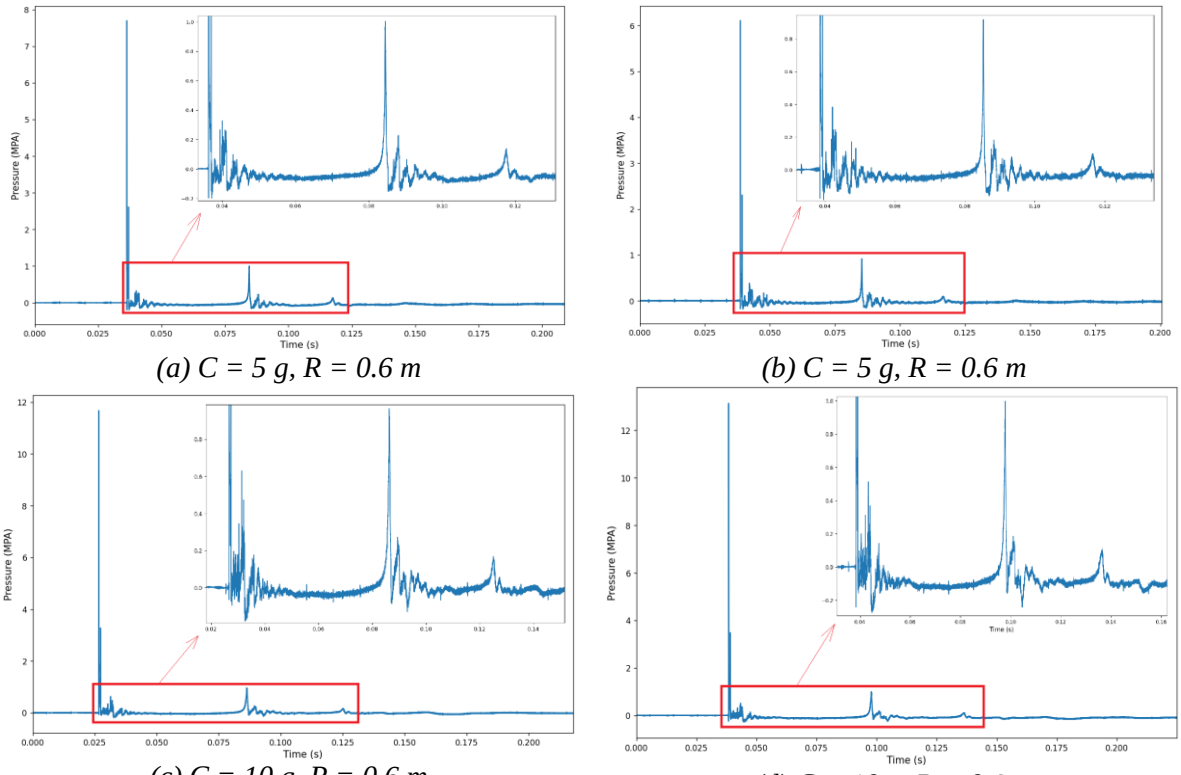

(a) C = 5 g, R = 0.6 m

(b) C = 5 g, R = 0.6 m

(c) C = 10 g, R = 0.6 m

(d) C = 10 g, R = 0.6 m

Fig. 4. Measured data of underwater shockwave pressure.

4.4.2. Denoising process

The procedures of processing and connecting signal segments are shown in Fig. 5 as follows: Calculate the forward and backward derivatives of the entire original signal

to check the filtering conditions for J_i and P_i (corresponding to ith sharp jump and ith sharp peak), so that the initial signal is divided into even and odd segments, odd segments are denoised with CEEMDAN (except that the first segment is processed by EMD), even segments are denoised with EMD. The result after the filtering process of a typical signal is shown in Fig. 6, including 5 segments. The denoising signal of the odd segment is taken as the root, then the beginning point and the end point of the 2 even signal segments after and before it are correspondingly connected to points of this odd signal segment, obtaining the denoised signal.

In Fig. 5, $S(t)$ is the original signal, J_i and P_i are the points that are considered as the beginning of the i^{th} sharp pressure jump, and the i^{th} sharp peak pressure, respectively; $S_{2i\text{-}1}$, S_{2i} are the consecutive odd and even signal segments divided by points J_i and P_i, respectively; $\overline{S_i(t)}$ is the i^{th} denoised signal.

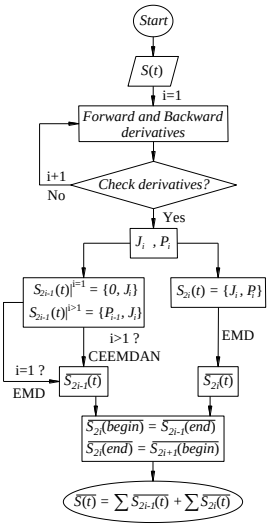

Fig. 5. Flow chart of denoising signal.

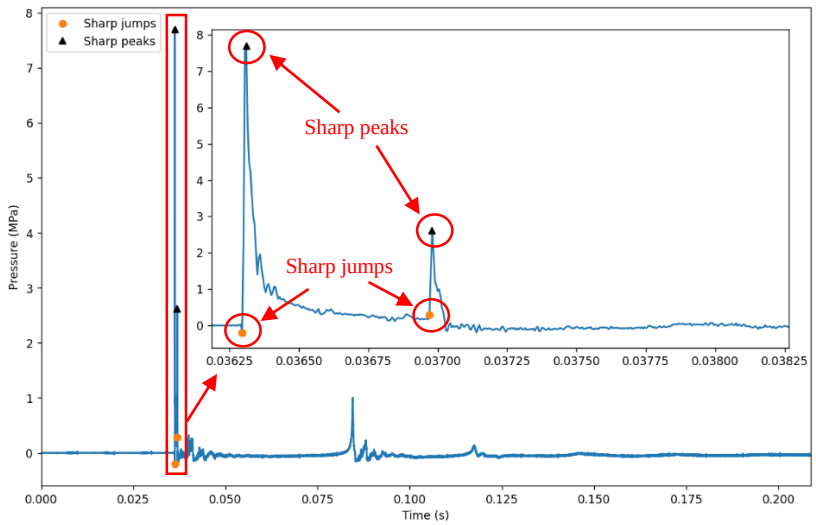

Fig. 6. Sharp jumps and sharp peaks split the original signal into 5 pieces.

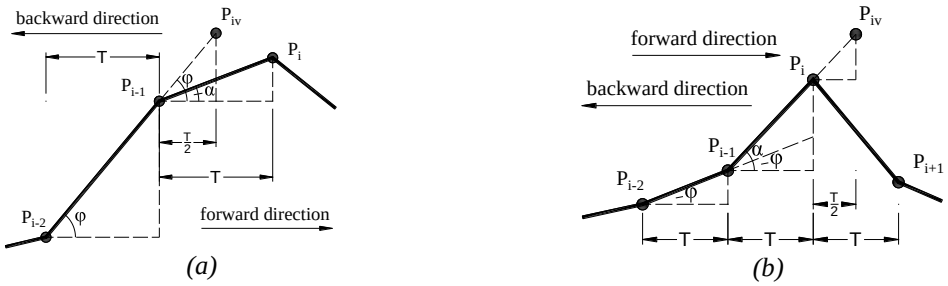

Fig. 7. Virtual sharp peaks for 2 circumstances $\varphi > \alpha$ (a) and $\varphi < \alpha$ (b).

The first odd signal only takes the residue to determine the trend line of the signal, so EMD is chosen for the decomposing process because the residue obtained from it is much faster than that of CEEMDAN, while still being effective for signal types that do

not have sudden changes in amplitude. The reason for using EMD for even signal segments is similar. Sharp peaks from the 2nd odd section onward are as likely as not accurate peaks because the sampling rate causes the measurement instrument to miss the time when the peaks occur. Assuming that the sampling rate is decreased twice, Fig. 7 illustrates a method determining a virtual peak P_{iv} from a measured peak P_i at a previous time of half frequency and 2 previous nearest signal points (P_{i-1} and P_{i-2}), including 2 circumstances $\varphi > \alpha$ (Fig. 7a) and $\varphi < \alpha$ (Fig. 7b), then CEEMDAN will take into account the former to decompose instead of the latter, 50 groups of Gaussian white noises with a standard deviation of 0.2 are added, and the maximum number of sifting iterations is set to 100.

IMFs of segments 3 and 5 are shown in Fig. 8.

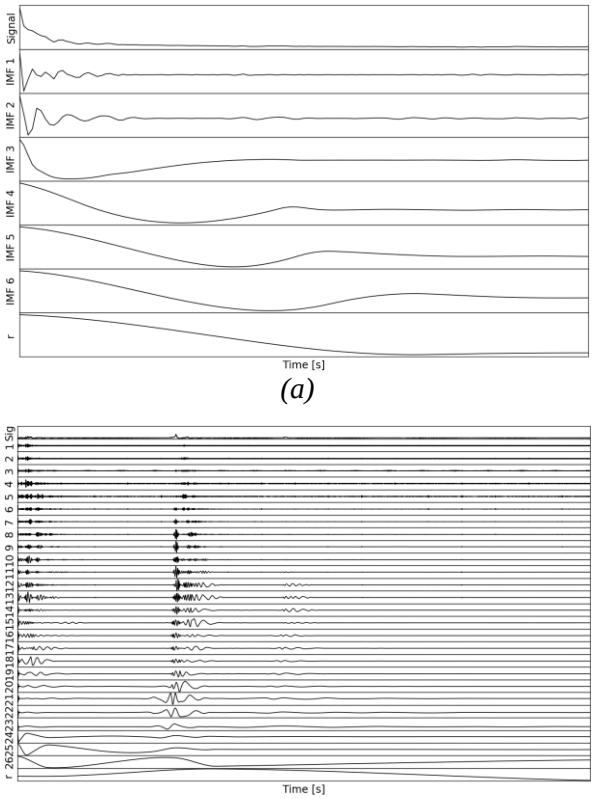

The residue and some extracted IMFs from Fig. 8 are combined to reconstruct, obtaining the denoised signal as the expression below:

$$\bar{S} = r + \sum_{i=0}^{k} IMF_{k-i} \quad (9)$$

where $\bar{S}$ is the denoised signal, r is the residue of the original signal, k is the total number of IMFs extracted from the original signal, i is the number of eliminated IMFs. From expression (9), it can be seen that the IMFs that are prioritized for retention have indexes ranging from high to low. Formula (9) is also the target denoising model.

Fig. 8. IMFs and residual of signal section 3 (a) and section 5 (b).

4.4.3. The evaluation of the denoising efficiency

The denoising efficiency of the denoised signal obtained by (9) is evaluated with 3 measurements: The signal-to-noise ratio (SNR), mean squared error (MSE) of the signal before and after the denoising process, and the average curvature of the denoised curve

as presented in section 3. Especially, the first two measurements are determined as (10) and (11), the last one is determined as (5) in section 3:

$$SNR = 10\log_{10}\left(\frac{\sum_{i=1}^{L}(S_i)^2}{\sum_{i=1}^{L}(S_i - \bar{S}_i)^2}\right) \tag{10}$$

$$MSE = \frac{1}{L}\sum_{i=1}^{L}(\bar{S}_i - S_i)^2 \tag{11}$$

where S_i and $\bar{S}_i$ are the amplitude of underwater shockwave pressure of the i^{th} signal point of the original signal and the denoised signal, respectively; L is the signal length (corresponding to the total number of signal points); SNR reflects the energy relationship between noise and desired signal, the larger the SNR, the better the signal quality, indicating that the signal level is greater than the noise level. On the other hand, MSE reflects the average energy of noise, so the smaller MSE is, the better the noise reduction effect.

4.4.4. Denoising results

The denoising efficiency obtained from recombinations is expressed by evaluation indices. Three evaluating indices (Curvature, SNR, MSE) are calculated as Eq. (5), Eq. (10), and Eq. (11) for the signal obtained from Eq. (9) when every number of eliminated IMFs is chosen (corresponding to i in Eq. (9)), they are scaled into a closed interval from 0 to 1 for ease of evaluation and visualized in Fig. 9.

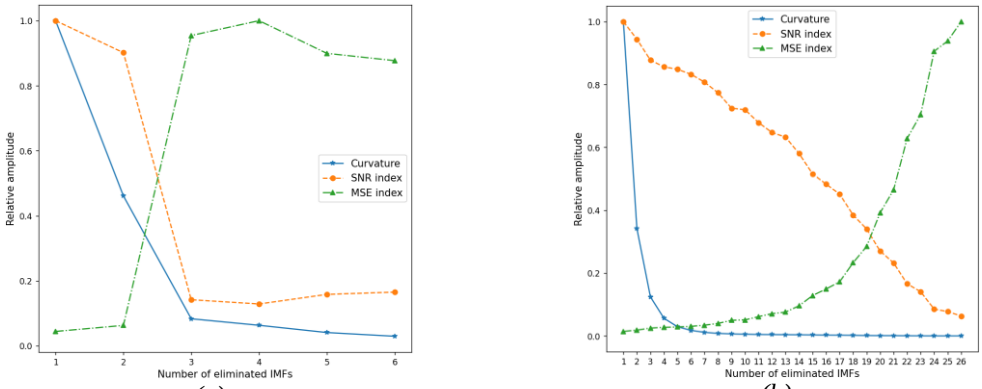

(a) *(b)*

Fig. 9. The relationship graph among 3 evaluation indices (Curvature, SNR, MSE) of segment 3 (a) and segment 5 (b), corresponding to each increase of i in Eq. (9).

Figure 9 shows that, along with the increased number of eliminated IMFs, SNR has a trend of almost linear decrease in general, representing that the denoising model should eliminate IMFs as little as possible. The 2 remaining indices are inversely proportional,

so the chosen number of eliminated IMFs should be the intersection of 2 connecting lines of these indices. Fig. 9(a) indicates that the recombination except the two first IMFs is the best denoising model for the signal segment 3. For Fig. 9(b), the option of choosing 5 eliminated IMFs is the suitable denoising model for the signal segment 5.

5. Evaluation and discussion

The application results of the two denoising models above are shown in Fig. 10. Intuitively observing from Fig. 10 witnesses a bright result of the denoising efficiency. Specifically, positive phase waveforms of the incident wavefront and gas bubbles (magnified from red frames) are zoomed sequentially from left to right for a clear observation. It can be seen that noises in the original signal are significantly eliminated while its waveform is still preserved. For further analysis, the comparison of quantitative results between the original signal and its denoised result is shown in Table 2.

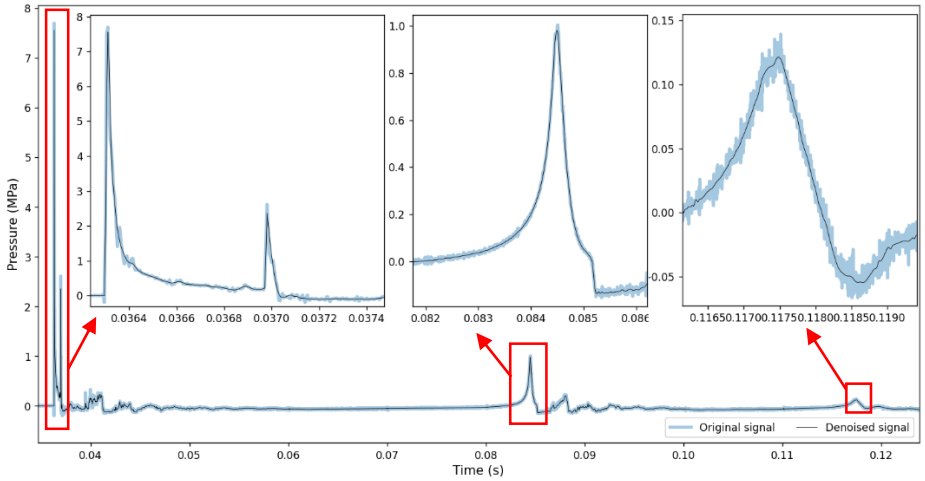

Fig. 10. The denoising result visualization of the typical signal.

Table 2. Peak comparison between the original signal and its denoised result

Shockwave and pulsations	Original signal (MPa)	Denoised signal (MPa)	Difference (%)
Incident wavefront	7.697 2.613	7.549 2.353	1.92 9.95
1st gas bubble	1.005	0.980	2.49
2nd gas bubble	0.139	0.121	12.94

The quantitative comparison results of peak pressure values for incident waves and gas bubbles are listed in Table 2. For the incident wave, the p_{max} value obtained from the denoised signal is 7.594 MPa, compared with the p_{max} value from the original signal in this section is 7.697 MPa, the difference is only 1.92%. Along with that, the fluctuations in the original signal are almost completely eliminated, so a smooth waveform is exposed. Furthermore, it

is possible to calculate easily the positive phase duration and pulse of the blasting load from the denoising result because the zero-crossing point of the denoised signal waveform can be easily found, which is very difficult to determine for the original signal.

6. Conclusion

Water is a sensitive environment to all disturbances caused by surrounding sources, so the measured signal of shockwave pressure of an underwater explosion contains a lot of noise, causing waveform distortion. Especially the incident wave, where a very large pressure amplitude occurs in an extremely short time, combined with the complex law of pressure drop in the water environment, this covers the characteristics of the original signal, making it difficult to further analyze the phenomena created when blasting underwater.

This article uses the EMD-CEEMDAN algorithm, combined with python programming tricks to split the original signal into pieces for separately denoising purposes, avoiding the end effect phenomenon that often occurs when using the EMD algorithm family, thereby a suitable noise reduction model is established. The applied criteria are the curvature of the denoised signal spline, SNR, and MSE, which are calculated to consider and evaluate the denoising effect, obtaining an effectively denoised signal of underwater shockwave pressure.

The proposal of authors: The results obtained from this article make it possible to calculate further parameters of an underwater blasting load such as the positive phase duration and the blasting pulse, which are difficult to do when using the original signal. Simultaneously, the pressure curve from this article can be completely considered as a dynamic load to be included in calculation software based on the finite element method such as SAP2000, ETABS, and VN3DPro, etc. to calculate the behavior of the structure when subjected to this type of load.

Acknowlegment

This article uses data that is provided and supported by the national-level project of the Socialist Republic of Vietnam, code: 32/18-C-ĐTĐL.CN.CNC [9].

References

[1] Hồ Sĩ Giao, Đàm Trọng Thắng, Lê Văn Quyển, Hoàng Tuấn Chung, *Nổ hóa học lý thuyết và thực tiễn*. Nxb Khoa học tự nhiên và Công nghệ, 2010.

[2] Đàm Trọng Thắng, Bùi Xuân Nam, Trần Quang Hiếu, *Nổ mìn trong ngành mỏ và công trình*. Nxb Khoa học tự nhiên và Công nghệ, 2015.

[3] G. Barras, M. Souli, N. Aquelet, N. Couty, "Numerical simulation of underwater explosions using an ALE method, the pulsating bubble phenomena", *Ocean Engineering*, Vol. 41, pp. 53-66, 2012. DOI: 10.1016/j.oceaneng.2011.12.015

[4] S. S. Emamzadeh, M. T. Ahmadi, S. Mohammadi, M. Biglarkhani, "Dynamic adaptive finite element analysis of acoustic wave propagation due to underwater explosion for fluid-structure interaction problems", *Journal of Marine Science and Application*, Vol. 14, pp. 302-315, 2015. DOI: 10.1007/s11804-015-1322-x

[5] C. Huang, M. Liu, B. Wang, Y. Zhang, "Underwater explosion of slender explosives: Directional effects of shock waves and structure responses", *International Journal of Impact Engineering*, Vol. 130, pp. 266-280, 2019. DOI: 10.1016/j.ijimpeng.2019.04.018

[6] R. Kicínski, B. Szturomski, "Pressure Wave Caused by Trinitrotoluene (TNT) Underwater Explosion-Short Review", *Journal of Applied Sciences*, Vol. 10(10), 2020. DOI: 10.3390/app10103433

[7] Y. X. Peng, A. M. Zhang, F. R. Ming, "Numerical simulation of structural damage subjected to the near-field underwater explosion based on SPH and RKPM", *Journal of Ocean Engineering*, Vol. 222, 2021. DOI: 10.1016/j.oceaneng.2021.108576

[8] S. Beji, A. Tatlisuluoglu, "Blast Pressure Measurements of an Underwater Detonation in the Sea", *Journal of Marine Science and Application*, Vol. 20, 2021, pp. 706-713. DOI: 10.1007/s11804-021-00230-1

[9] Đàm Trọng Thắng và những người khác, Đề tài KHCN độc lập cấp quốc gia mã số: 32/18-C-ĐTĐL.CN.CNC, 2022.

[10] Đàm Trọng Thắng, Trần Đức Việt, Nguyễn Phú Thắng, "Sự biến đổi của sóng nổ tại mặt phân cách giữa giữa môi trường nước và môi trường nước chứa bóng khí", *Tạp chí Nghiên cứu khoa học và Công nghệ quân sự*, số 70, tr. 139-145, 2020.

[11] Đàm Trọng Thắng, Trần Đức Việt, "Nghiên cứu ảnh hưởng của màn chắn bóng khí đến trường sóng nổ lan truyền trong môi trường nước", *Tạp chí Khoa học kỹ thuật Mỏ - Địa chất*, số 62, kỳ 5, 2021.

[12] M. Sun, L. Wu, C. Li, Q. Yuan, Y. Zhou, X. Ouyang, "Smooth model of blasting seismic wave signal denoising based on two-stage denoising algorithm", *Journal of Geosystem Engineering*, Vol. 23, Iss. 4, pp. 234-242, 2020. DOI: 10.1080/12269328.2020.1778543

[13] Y. Peng, Y. Liu, C. Zhang, L. Wu. "A Novel Denoising Model of Underwater Drilling and Blasting Vibration Signal Based on CEEMDAN", *Arabian Journal for Science and Engineering*, Vol. 46, pp. 4857-4865, 2021. DOI: 10.1007/s13369-020-05274-z

[14] Z. Liu, Y. Peng, "Study on Denoising Method of Vibration Signal Induced by Tunnel Portal Blasting Based on WOA-VMD Algorithm", *Journal of Applied Sciences*, Vol. 13, Iss. 5, 2023. DOI: 10.3390/app13053322

[15] R. Bracewell, *The Fourier Transform and Its Applications*, 3rd ed., McGraw-Hill Publisher, 1999.

[16] R. E. Kalman, "A new approach to Linear Filtering and Prediction problems", *Journal of Basic Engineering*, Vol. 82(1), pp. 35-45, 1960. DOI: 10.1115/1.3662552

[17] G. Welch, G. Bishop, *An introduction to the Kalman filter*. University of North Carolina, 2006.

[18] Wavelet Toolbox™. MATLAB®. MathWorks®

[19] N. E. Huang, Z. Shen, S. R. Long et al., "The empirical mode decomposition and the Hilbert spectrum for nonlinear and non-stationary time series analysis", *Proceedings: Mathematical, Physical and Engineering Sciences*, Vol. 454, pp. 903-995, 1998. http://www.jstor.org/stable/53161

[20] M. E. Torres, M. A. Colominas, G. Schlotthauer, P. Flandrin, "A complete ensemble empirical mode decomposition with adaptive noise", *2011 IEEE International Conference on Acoustics, Speech and Signal Processing (ICASSP)*, 2011. DOI: 10.1109/ICASSP.2011.5947265

[21] R. H. Cole, *Underwater explosions*. Princeton University Press: Princeton, NJ, USA, 1948.

[22] L. Li, Y. You, "Time-frequency energy analysis of deepwater explosion shock wave signals based on HHT", *2020 2nd International Conference on Computer Science Communication and Network Security, MATEC Web of Conferences*, Vol. 336, 2021. DOI: 10.1051/matecconf/202133601017

KHỬ NHIỄU TÍN HIỆU ĐO ÁP LỰC SÓNG NỔ DƯỚI NƯỚC DỰA TRÊN EMD-CEEMDAN CÓ XÉT TỚI ĐỘ CONG CỦA ĐƯỜNG CONG TÍN HIỆU

Vũ Tùng Lâm[1,*], Đàm Trọng Thắng[1], Trần Đức Việt[2]

[1]*Trường Đại học Kỹ thuật Lê Quý Đôn, Hà Nội, Việt Nam*

[2]*Tổng cục Công nghiệp quốc phòng, Hà Nội, Việt Nam*

Tóm tắt: Tín hiệu đo áp lực sóng nổ của một vụ nổ dưới nước thường bị gây nhiễu bởi nhiều yếu tố khách quan như sự nhiễu động của môi trường xung quanh các cảm biến, sự phức tạp của truyền sóng và phản xạ sóng trong môi trường, sự hình thành và dao động của các khoang bóng khí, đặc biệt là đặc trưng tín hiệu analog luôn tồn tại nhiễu do ảnh hưởng của nhiễu điện tử đến từ bộ chuyển đổi dòng điện A/D và sai số bảng mạch nhúng trong thiết bị đo… Đây là những nguyên nhân chính gây ra biến dạng dạng sóng ban đầu, làm che phủ các đặc trưng quan trọng của tín hiệu, gây khó khăn trong việc sử dụng và phân tích sâu thêm về áp lực sóng nổ dưới nước. Trên cơ sở hai thuật toán phân tách dạng thực nghiệm (EMD) và phân tách dạng thực nghiệm tổng hợp hoàn chỉnh với nhiễu thích ứng (CEEMDAN), bài báo thiết lập kết hợp cả hai thuật toán trên vào một mô hình khử nhiễu gọi là EMD-CEEMDAN bằng mã lập trình python. Ba tiêu chí đánh giá là độ cong trung bình của đường cong tín hiệu, tỉ số tín hiệu trên nhiễu (SNR) và sai số bình phương trung bình (MSE) được sử dụng để chọn ra mô hình khử nhiễu tín hiệu hợp lý nhất. Áp dụng mô hình khử nhiễu tìm được cho bộ tín hiệu thí nghiệm đo áp lực nổ dưới nước nhận được kết quả là loại bỏ được nhiễu tần số cao, đưa tín hiệu về dạng đặc trưng sóng nổ trơn trong khi áp lực đỉnh chỉ chênh lệch khoảng 2% so với tín hiệu ban đầu.

Từ khóa: *Nổ dưới nước; khử nhiễu; EMD; CEEMDAN.*

Received: 01/10/2023; Revised: 20/12/2023; Accepted for publication: 27/12/2023

❑